American Journal of Electromagnetics and Applications
2016; 4(2): 39-49
http://www.sciencepublishinggroup.com/j/ajea
doi: 10.11648/j.ajea.20160402.15
ISSN: 2376-5968 (Print); ISSN: 2376-5984 (Online)

Corrosion Performance of Copper - Diamond Composites in Different Aqueous Solutions

Z. Abdel Hamid[1, *], Mona H. Gomaa[1], H. B. Hassan[2]

[1]Corrosion Control and Surface Protection Laboratory, Central Metallurgical Research & Development Institute, CMRDI, Helwan, Cairo, Egypt

[2]Faculty of Science, Department of Chemistry, Cairo University, Giza, Egypt

Email address:

forzeinab@yahoo.com (Z. A. Hamid), Hanaa20055@hotmail.com (H. B. Hassan)

[*]Corresponding author

To cite this article:

Z. Abdel Hamid, Mona H. Gomaa, H. B. Hassan. Corrosion Performance of Copper - Diamond Composites in Different Aqueous Solutions. *American Journal of Electromagnetics and Applications.* Vol. 4, No. 2, 2016, pp. 39-49. doi: 10.11648/j.ajea.20160402.15

Received: December 9, 2016; **Accepted**: December 23, 2016; **Published**: January 20, 2017

Abstract: In the present work copper/diamond composites, such as (Cu-10 V_f% diamond uncoated, Cu-30 V_f % diamond uncoated, Cu-10 V_f % diamond coated NiCrB and Cu-30 V_f % coated NiCrB) as heat sink materials have been fabricated using powder metallurgy and electroless techniques. The copper powder used in this study has been fabricated using electroless technique and the diamond powder was electroless coated with NiCrB film. The copper powder have been mixed with the uncoated or coated diamond particles, milled, compacted and sintered at 900°C in a hydrogen atmosphere. The corrosion behavior of the copper composite samples has been investigated in 0.6 M NaCl, 0.1 M HCl and 0.5 M NaOH solutions using potentiodynamic polarization anodic and cathodic Tafel lines and electrochemical impedance spectroscopy (EIS). Scanning electron microscopy (SEM) linking with energy dispersive X-ray spectroscopy (EDS) has been used to investigate the surface morphology and the chemical composition of the coated layer. The results of the corrosion test illustrated that the coated and uncoated Cu/diamond composites suffer from corrosion to a different extent in various electrolytes. The lowest corrosion rate in all the studied media was recorded for Cu-10 V_f % D coated NiCrB composite compared with the massive copper or uncoated composite samples.

Keywords: Metal-Matrix Composites (MMCs), Particle-Reinforced Composites, Corrosion, Scanning Electron Microscopy (SEM), Powder Processing, Sintering

1. Introduction

Copper and copper alloys are the most versatile engineering materials available. The combination of physical properties such as strength, conductivity, outstanding resistance to corrosion and fatigue, machinability and ductility makes copper suitable for a wide range of application. These properties can be further enhanced with variations in the composition and manufacturing methods [1, 2]. Copper, brass, bronze and copper-nickel alloy are used extensively for automotive radiators, heat exchangers, home heating systems, solar collectors, and various other applications requiring rapid conduction of heat across or along a metal section. Because of their outstanding ability to withstand corrosion, they are also used for pipes, valves and fittings in systems carrying potable water, process water or other aqueous fluids, and industrial gases. Additionally, for many decades, copper metal gain a great attention as a heat sink material for semiconductor electronic packages [3]. A heat sink is a passive heat exchanger that cools a device by dissipating heat within a solid material into the surrounding medium such as air or liquids. Heat sinks also help to cool electronic and optoelectronic devices, such as high-power lasers and light emitting diodes (LEDs) [3, 4]. Copper is also used since it has around twice the conductivity of aluminum, but is three times as heavy as aluminum and it has the highest thermal conductivity among metals [5]. Unfortunately, copper has become a bottleneck in removing heat from semiconductor devices, and its thermal conductivity is insufficient to dissipate the heat generated from the new generation of semiconductor components [5-7].

Recently, the development of the metal matrix composites (MMC's) is a very important issue to meet the critical performance requirement for advanced engineering applications. Copper– diamond composites are expected to combine a high thermal conductivity with a coefficient of thermal expansion (CTE) close to that of semiconductor materials. The thermal conductivity and CTE of these composites can be easily controlled by modifying their compositions. However, due to the lack of mutual wetability and insolubility, a very weak bonding between diamond and pure copper matrix is formed in the consolidated composite. It is well-known that ceramic materials are frequently not wetted by liquid metals, so, many research investigators have tried to overcome the problems of non wetability of diamond with metals to enhance the interaction at the metal/diamond interface by using different means such as the addition of elements to the liquid metal (oxidation) [8], surface fluxes [9], the use of metal coating [10, 11], or heat treatment of ceramic particles [12].

The corrosion performance of metals and alloys in aggressive media depends on many factors such as the chemical composition [13]. The corrosion products of copper and its inhibition in a variety of media, especially when it has chloride ions have a harmful effect on the heat transfer, causing a decrease in heating and cooling efficiency of the equipment [14-20]. The mechanism of copper and copper based alloys electro-dissolution in chloride media has been investigated by Milić et al. [21]. Moreover, it is generally accepted that the anodic dissolution of copper is influenced by a chloride concentration independently of pH [22 -24].

In recent years, several studies have been performed to enhance the thermal conductivity and the coefficient of thermal expansion (CTE) properties of Cu/diamond composite [11]. However, very few studies have reported the corrosion resistance of Cu- composite, and these studies generally for predicting the structural failure of the Cu/composite compared with pure Cu. The electrochemical corrosion performance of copper at the micro scale still requires a further investigation. So, the present work aims at evaluating the corrosion behavior of Cu-diamond composites uncoated and coated with electroless NiCrB compared with massive Cu by using potentiodynamic polarization Tafel lines and electrochemical impedance spectroscopy (EIS) measurements in different aqueous solutions of 0.6 M NaCl, 0.1 M HCl and 0.5 M NaOH.

2. Experimental Procedures

2.1. Fabrication of Cu/diamond Composites

Cu/diamond composites were fabricated using powder metallurgy technique. The grain sizes of the investigated diamond powders were ranged from 20 to 40 μm, type RVD and were supplied by (Polaris Diamond Powder Co., Ltd). The diamond powder was electroless coated with NiCrB film. Copper powder used in this study has been fabricated using electroless technique.

The diamond surface must be treated before electroless coating using 50% HNO_3 solution and activated using palladium chloride solution to improve the coating adhesion. The chemical composition and the operating conditions to prepare the diamond coatings with NiCrB layer were presented in Table 1. In these solutions, nickel sulphate and chromium acetate are the main source of nickel and chromium metals, respectively, sodium acetate salt acts as a complexing agent, and dimethyl amine borane (DMAB) acts as a reducing agent. At the operating temperature, the calculated amount of the reducing agent was added to the plating solution, the pH of the solution was adjusted and the stationary weight percent of the diamond powders was added. The coated powder was filtrated, washed with distilled water and then dried.

In order to prepare Cu/diamond composites, the copper powders were mixed with the diamond particles then milled for 20 min, compacted under the pressure of 100 bar then sintered at 900°C for 1 hr using hydrogen atmosphere.

Table 1. *Chemical composition and the operating condition of electroless plating solutions for diamond particles coated by NiCrB layer.*

Composition	Concentration, g l^{-1}
Nickel acetate	6
Chromium acetate	40
Sodium acetate	65
Dimethyl amine borane (DMAB)	3
Operating condition	
Temperature, °C	85-90
pH	4.5
Time, h.	2

2.2. Analysis and Characterizations

Scanning electron microscope (SEM) linking with energy dispersive X-ray spectroscopy (EDS) detector attachment, model JEOL, JSM-5410, were used to investigate the surface morphology and the compositions of the various Cu/diamond composites.

2.3. Electrochemical Measurements

The corrosion study was carried out using potentiodynamic polarization anodic and cathodic Tafel lines and electrochemical impedance spectroscopy (EIS). The electrochemical measurements were performed using IviumStat instrument (supplied by Ivium Technologies, Eindhoven, the Netherlands). The IviumSoft software can be used to control IviumStat instrument with a personal computer (PC). The personal computer (PC) is used to specify the parameters of the measurement, to display the measured curves and to calculate the results of the measurements. Prior to the corrosion test, the surface of specimens was polished mechanically with silicon carbide papers of different grades, rinsed with acetone and dried. The electrochemical measurements were performed on rectangular specimens as working electrodes; each has a geometric surface area of 1.0 cm^2. The reference electrode that all potentials are referred was $Hg/Hg_2Cl_2/Cl^-$ saturated calomel electrode (SCE) of E_o = 0.240 V versus reference

hydrogen electrode (RHE) and the auxiliary electrode was a platinum sheet. The electrolytes used were 0.6 M NaCl, 0.1 M HCl and 0.5 M NaOH solutions prepared using triple distilled water. The polarization was started from the cathodic part and then the anodic part; first the electrode was put in the test solution till the open-circuit potential was reached (E_{corr}). The polarization was started from this point down to -0.5 V in the cathodic direction, and then, the polarization was reversed from the open-circuit potential up to +0.5 V in the anodic direction. The corrosion current (I_{corr}) was calculated from the intersection of the most linear parts of the anodic and cathodic lines at zero polarization. All experiments were carried out in aerated solutions at room temperature of 25 ± 1°C. On the other hand, the corrosion resistances of massive Cu and Cu- diamond composite electrodes were investigated using EIS measurements in 0.1 M HCl, 0.5 M NaOH, and 0.6 M NaCl solutions at OCP`s by applying a 10 mV sinusoidal potential through a frequency domain from 35 kHz down to 100 mHz. All experiments have been carried out in the test solutions at room temperature (25 ± 1°C).

3. Results and Discussion

The electrochemical behaviors of Cu and Cu- composites in 0.1 M HCl, 0.5 M NaOH and 0.6 M NaCl were carried out at the open-circuit potential using polarization Tafel lines and electrochemical impedance spectroscopy (EIS) at 25°C.

3.1. Corrosion Behavior in 0.1 M HCl Electrolyte

Representative Tafel lines for massive Cu, Cu- diamond uncoated composite and Cu-diamond coated NiCrB composite electrodes in 0.1 M HCl at 25°C at the open-circuit potential ($E_{o,}$) is shown in figure 1. A clear shift in the cathodic part of Tafel lines is observed for the Cu composite samples compared with massive Cu, but a slight shift is observed in the anodic part of Tafel lines. It is interesting to note a peak (I) in the anodic part of all Tafel lines for massive Cu and Cu composite samples at a polarization potential range of 0.19 - 0.22 V (SCE) followed by a slight decrease of the corrosion current density then it increases again. This peak could due to the dissolution of copper and the formation of an insoluble $CuCl_{ads}$ which could be adsorbed on the surface and retard the dissolution process, this species could be transformed into $CuCl^-_2$ in the presence of Cl^- according to the following equations [25-27]:

$$Cu + Cl^- \rightarrow CuCl + e^- \quad (1)$$

$$CuCl + Cl^- \rightarrow CuCl^-_2 \quad (2)$$

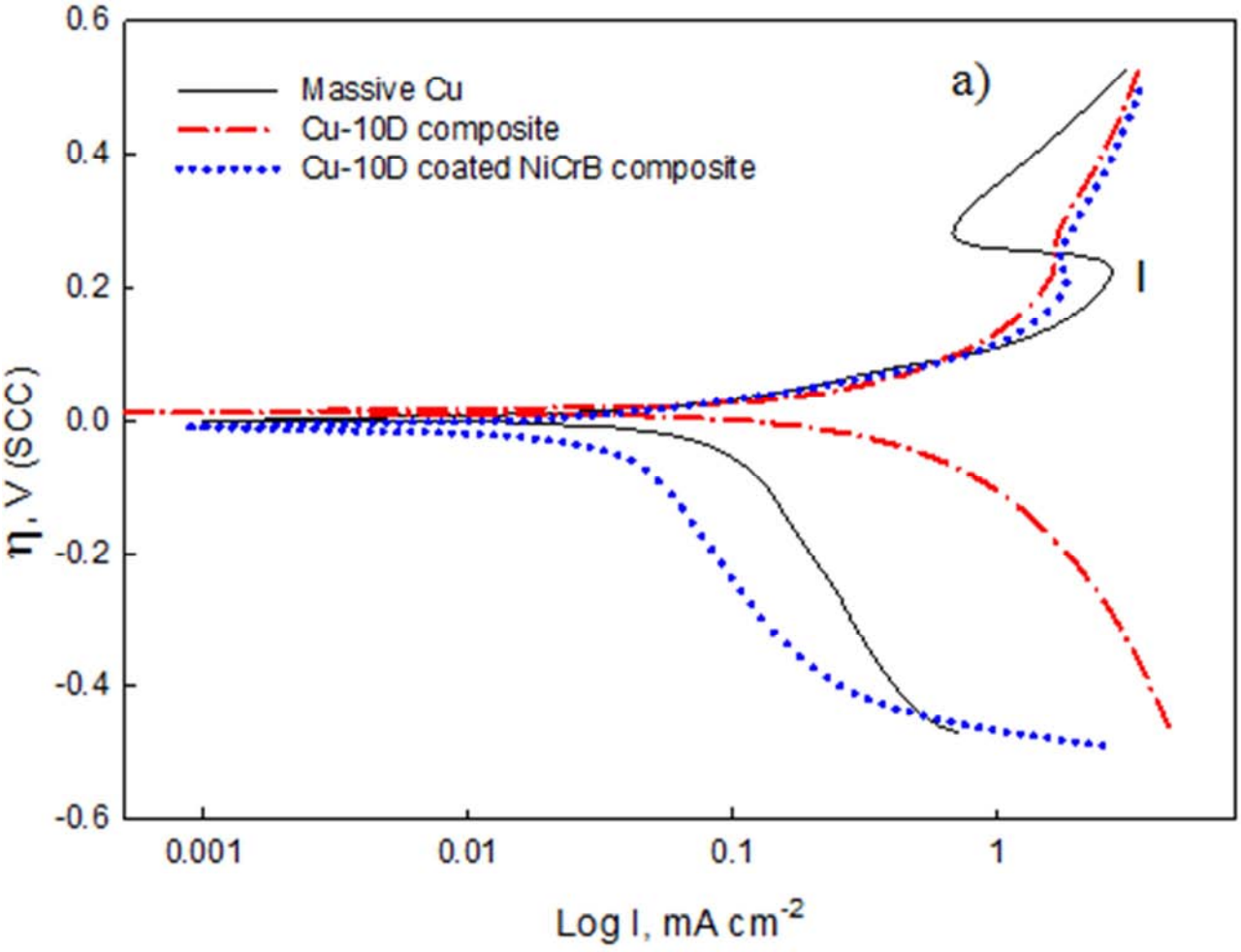

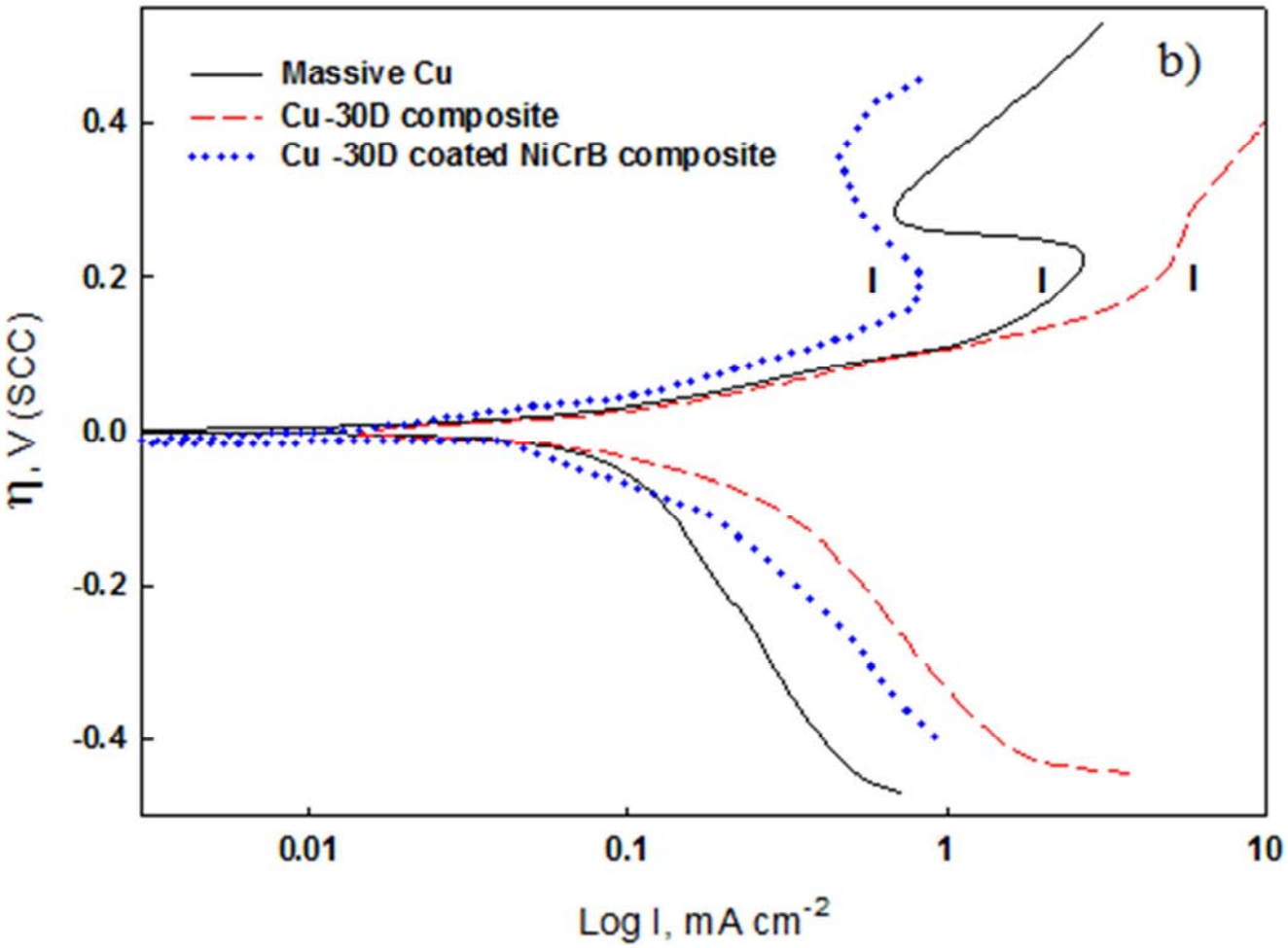

Figure 1. *(a, b). Polarization Tafel lines of Cu, Cu- diamond uncoated and coated NiCrB electroless composite samples in 0.1 M HCl at 1.0 mV s^{-1} at 25°C.*

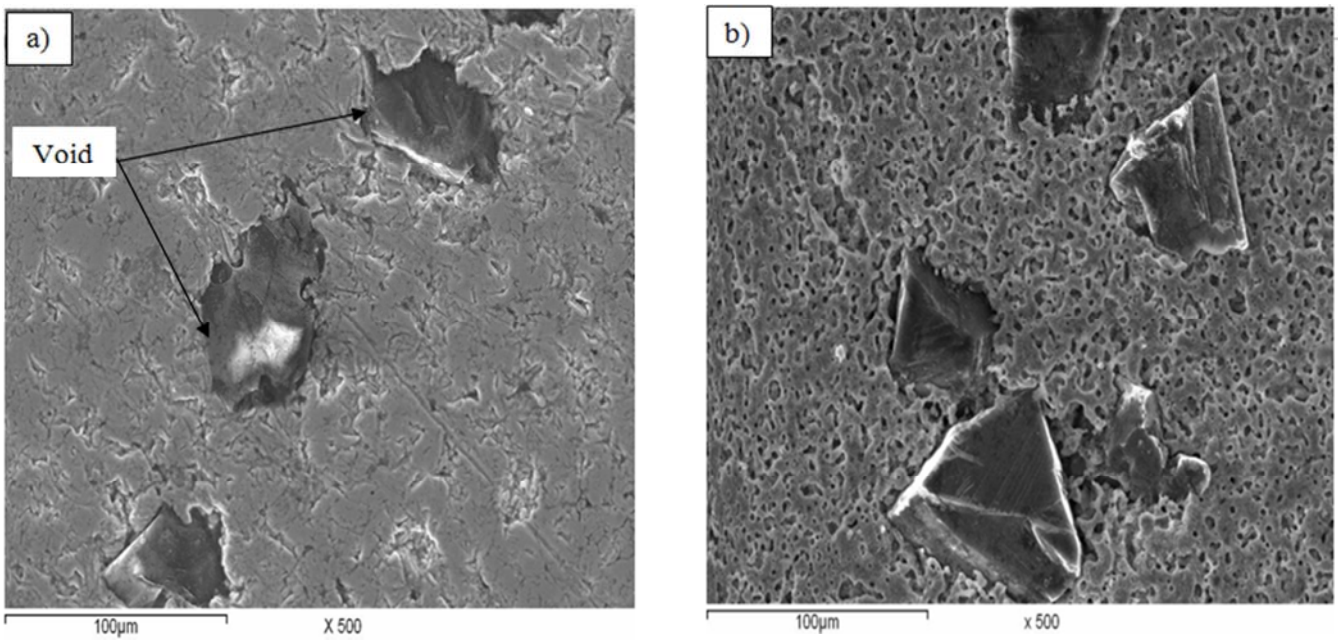

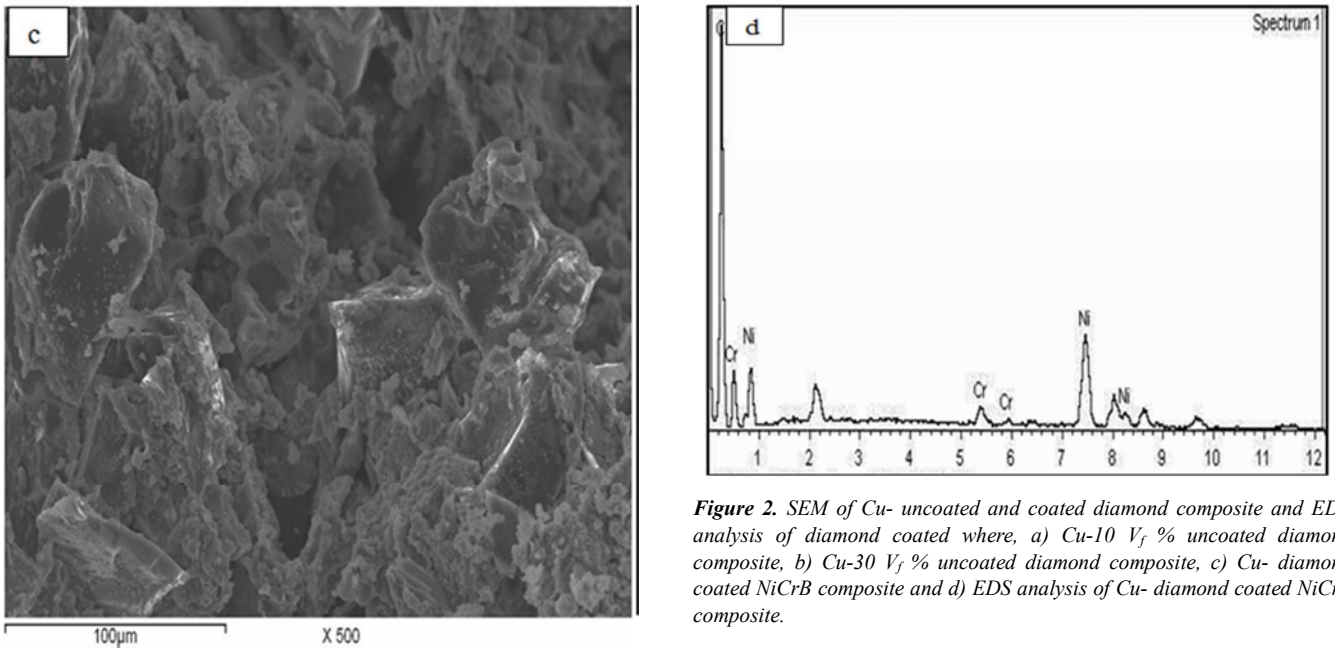

Figure 2. *SEM of Cu- uncoated and coated diamond composite and EDX analysis of diamond coated where, a) Cu-10 V_f % uncoated diamond composite, b) Cu-30 V_f % uncoated diamond composite, c) Cu- diamond coated NiCrB composite and d) EDS analysis of Cu- diamond coated NiCrB composite.*

Table 2. *Electrochemical parameters derived from Tafel lines for different Cu samples in 0.1 M HCl at 1.0 mV s^{-1} at 25°C.*

Sample	E_{corr}, V (SCE)	I_{corr}, (mA cm^{-2})	b_a, (V dec^{-1})	b_c, (V dec^{-1})	Corrosion rate (mpy)
Massive Cu	-0.05	0.089	0.114	-0.566	41.3
Cu-10D composite	-0.113	0.176	0.164	-0.456	81.6
Cu-30D composite	-0.059	0.189	0.103	-0.387	87.6
Cu-10D coated NiCrB	-0.079	0.04	0.207	-0.449	18.6
Cu-30D coated NiCrB	-0.219	0.07	0.111	-0.446	32.5

Moreover, Table 2 summarizes the electrochemical corrosion parameters including corrosion current density (I_{corr}), corrosion potential (E_{corr}) and anodic and cathodic Tafel slopes (b_a and b_c) that derived from the polarization curves of figure 1. The results indicate that massive Cu and the different Cu composite samples have suffered from corrosion to varying extents in 0.1 M HCl solution during the polarization test. The results revealed that a lower corrosion current density value was recorded for massive Cu compared with the Cu- uncoated diamond composite, this could due to that copper does not wet diamond well, which makes the production of Cu– diamond composites difficult and containing many voids. These voids increase with increasing the volume fraction (V_f %) of diamond in the composite (V_f 30 %) as shown in figure 2(a, b). This indicates that the general corrosion resistance of Cu is superior to that of the Cu- uncoated diamond. While, the corrosion current density of the Cu- diamond coated NiCrB composite is lower than that of Cu- diamond uncoated composites. These findings can be explained in the view of the good wettability of the coated diamond with Cu matrix (figure 2c). Moreover, the EDS analysis of the diamond coated with electroless NiCrB is illustrated in figure 2d. Our previous work [28] proved that the Cu- diamond coated NiCrB composite has a high transverse rupture strength (TRS) compared with that of Cu-diamond uncoated composite, and this finding was owing to the fact that the coated alloy acts as a barrier layer that decreases the pores at the interface and so it gives a good degree of adhesion which increases the strength of the final composite, reduces the voids and consequently improves the corrosion resistance (as shown in figure 2 c).

3.2. Corrosion Behaviour in 0.5 M NaOH Electrolyte

Figure 3 and Table 3 elucidate the effect of 0.5 M NaOH solution on the corrosion behavior of massive Cu, Cu-diamond uncoated composite and Cu- diamond coated NiCrB composite electrodes. Investigation of the polarization curves recorded in these experiments leads to a conclusion that an appreciable shift in the cathodic part of Tafel lines is observed, an anodic peak (I) is observed for massive Cu at a polarization potential of about 0.09 V, while two peaks (I, II) are observed in the anodic part of Tafel lines for Cu-10D composite samples at polarization potentials of about 0.11 and 0.4 V, respectively, while one peak is recorded for Cu-30D composite samples at a polarization potential of about 0.2 V, they followed by a slight decrease of the corrosion current density. Notably, the anodic polarization behavior of copper and copper composite depends on the polarization potential and it includes a transition from active to passive region with two anodic current peaks that include the formation of Cu_2O (peak I) film and a film that has $Cu(OH)_2$ and CuO (peak II) [29-32]. These oxidation products could adsorb on the electrode surface and prevent its further dissolution so, the (I_{corr}) decreases after these peaks [33]. From the results of the corrosion performance in 0.5 M NaOH (Table 3), it is clear that the corrosion rate of Cu-

uncoated diamond composite samples is slightly higher than that of massive Cu, while the corrosion rate of the Cu-diamond coated NiCrB composite samples is lower than that of massive Cu as well as the Cu- uncoated diamond composite samples. The correlation between the corrosion behavior and the surface morphology of Cu- diamond composite samples was carried out by investigating the morphology of the uncoated and coated surfaces (figure 2). As mentioned before the good wetability of the coated diamond with Cu matrix results in a homogenous surface with lower voids (figure 2c) which reduce the corrosion rate. Additionally, the relatively high corrosion rate of the Cu–diamond composite samples in 0.5 M NaOH is in agreement with Levy et al. [34].

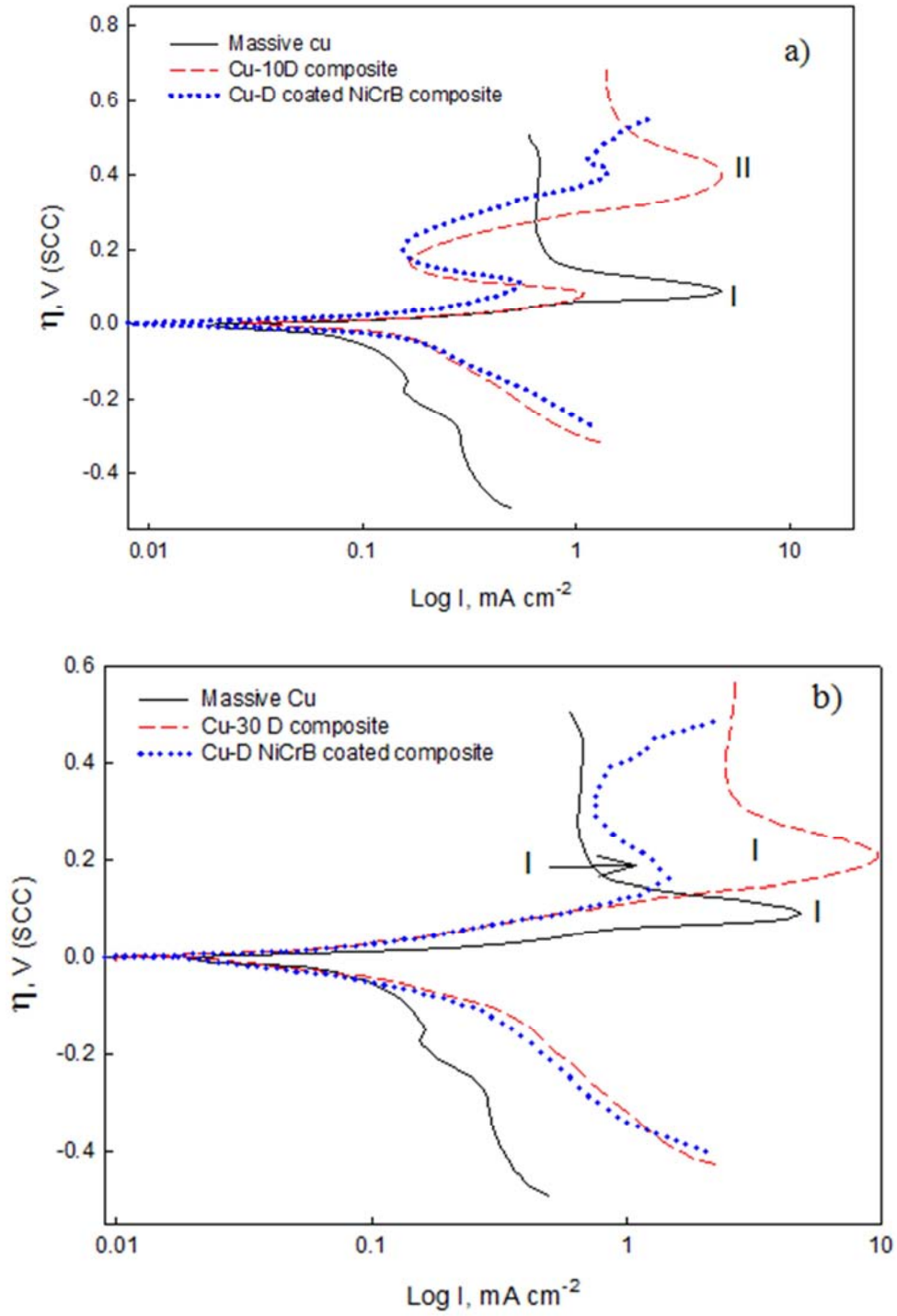

Figure 3. *(a, b). Polarization Tafel lines of massive Cu, Cu- diamond uncoated composite and Cu- diamond coated NiCrB composite electrodes in 0.5 M NaOH at 1.0 mVs^{-1} at 25°C.*

Table 3. *Electrochemical parameters derived from Tafel lines for different Cu samples in 0.5 M NaOH at 1.0 mV s^{-1} at 25°C.*

Sample	E_{corr}, V (SCE)	I_{corr}, (mA cm^{-2})	b_a, (V dec^{-1})	b_c, (V dec^{-1})	Corrosion rate (mpy)
Massive Cu	-0.266	0.130	0.038	-0.680	60.3
Cu-10D composite	-0.326	0.146	0.300	-0.341	67.7
Cu-30D composite	-0.304	0.16	0.199	-0.316	74.2
Cu-10D coated NiCrB	-0.289	0.110	0.316	-0.257	51
Cu-30D coated NiCrB	-0.205	0.147	0.109	-0.344	68.2

3.3. Corrosion Behavior in 0.6 M NaCl Electrolyte

The corrosion behavior of massive Cu and Cu– diamond composite samples was studied in 0.6 M NaCl at the open-circuit potential (E_o) and the results are presented in figure 4 and Table 4. Three distinct regions were observed in the Tafel lines, the active dissolution region, the active-passive transition region and the slight increase in the current region. In the active dissolution region an increase of current with potential is observed until the current reached the maximum value, after that, in the active-passive transition region, the current density declined rapidly with potential increase, forming an anodic current peak (I) that could due to the formation of unstable CuCl film and soluble chloride complexes ($CuCl_2^-$). Meanwhile, copper oxide and hydroxide can be formed. The anodic dissolution of Cu in chloride medium depends on the chloride ion concentration [35]. Chloride ions are very aggressive ions to copper and its composite, due to the tendency of the chloride ion to form an unstable film (CuCl) and soluble chloride complexes ($CuCl_2^-$) [36-38]. The results reveal a lower corrosion rate for all the Cu– diamond composite samples compared with massive Cu, but the Cu–diamond coated NiCrB composite samples exhibited much lower corrosion rate than the Cu- diamond uncoated composite samples. The insoluble corrosion products that formed on the surface may slow down the rate of anodic dissolution. Moreover, the reduction in the corrosion rate of the Cu-diamond uncoated composite compared with massive Cu could be attributed to the reduction in the active area of Cu exposed to the corrosive environment. On the other hand, the lowest corrosion rate obtained with Cu-diamond coated NiCrB composite could due to the reduction in the active area in addition to the surface homogeneity resulted from the good wetability of the coated diamond with Cu matrix.

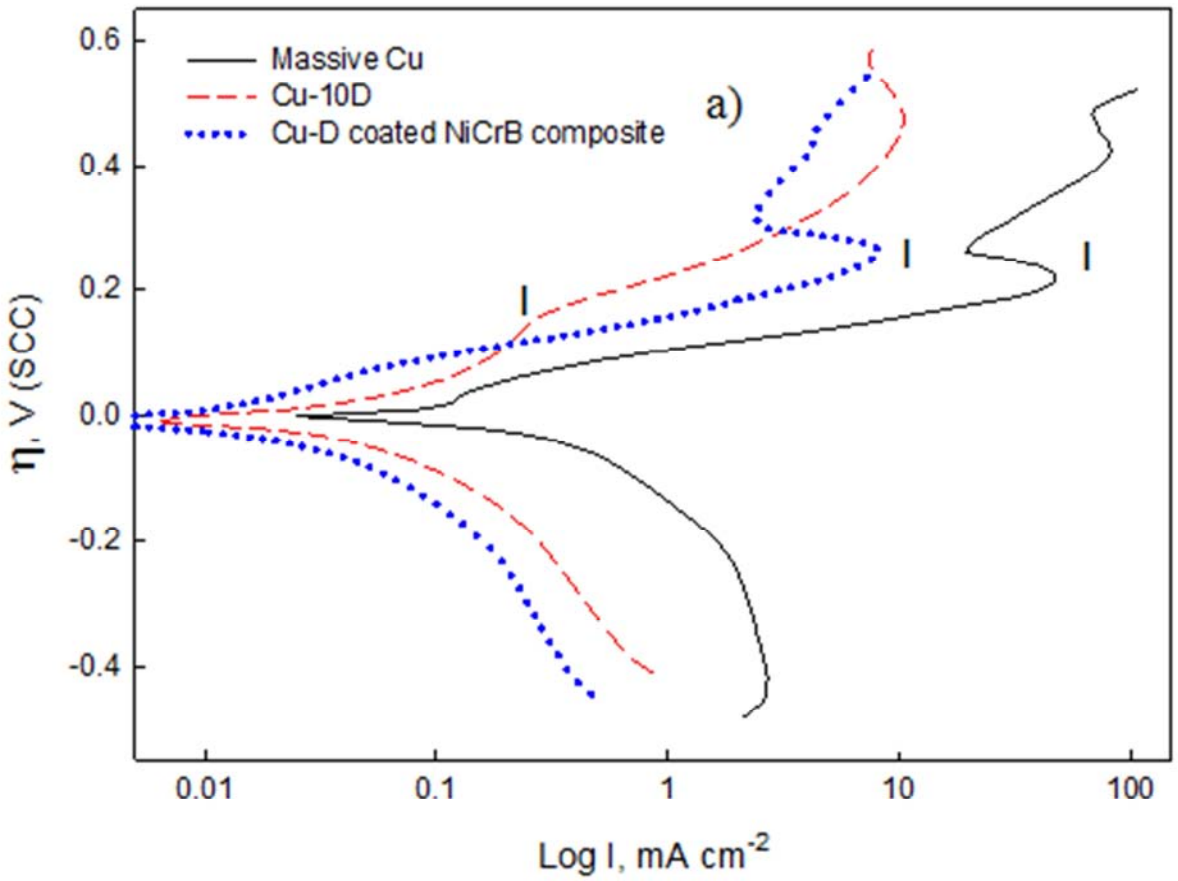

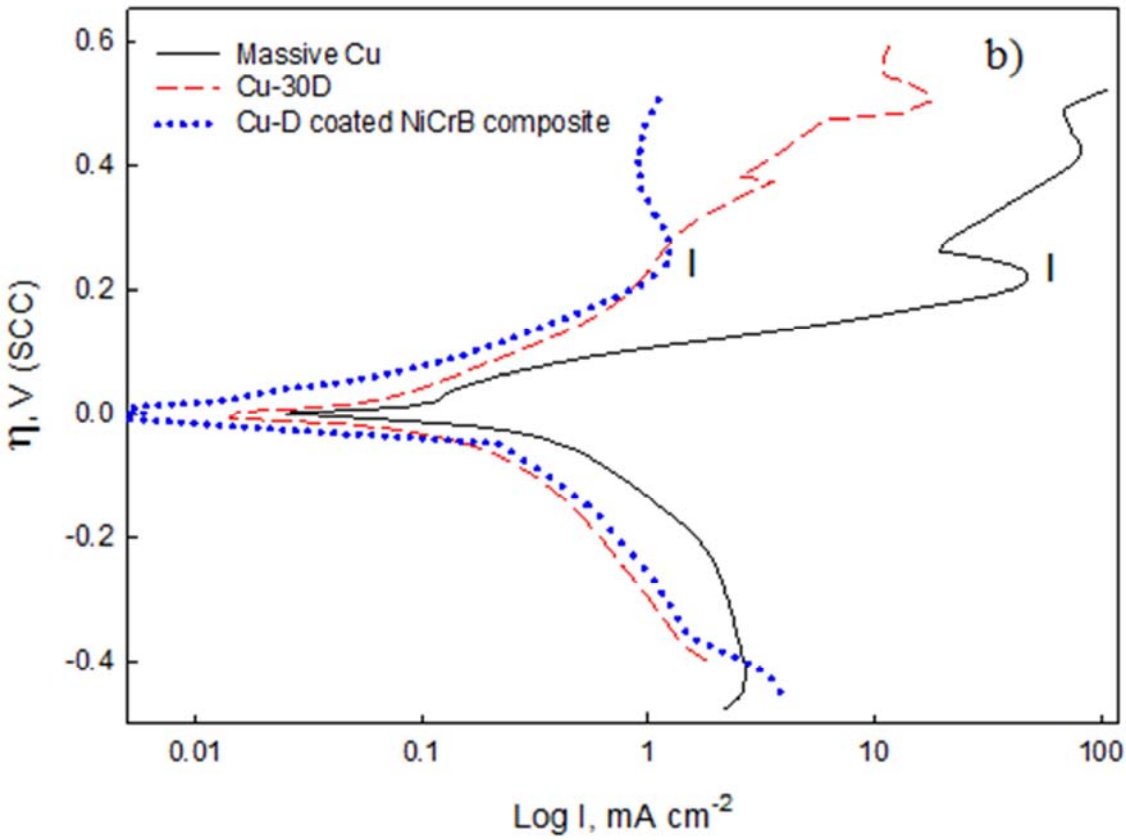

Figure 4. *(a, b). Polarization Tafel lines of Cu, Cu- diamond uncoated and coated NiCrB electroless composite samples in 0.6 M NaCl at 1.0 mV s^{-1} at 25°C.*

Table 4. *Electrochemical parameters derived from Tafel lines for different Cu samples in 0.6 M NaCl at 1.0 mV s^{-1} at 25°C.*

Sample	E_{corr}, V (SCE)	I_{corr}, (mA cm^{-2})	b_a, (V dec^{-1})	b_c, (V dec^{-1})	Corrosion rate (mpy)
Massive Cu	-0.229	0.20	0.062	-0.516	92.7
Cu-10D composite	-0.230	0.10	0.197	-0.426	47.5
Cu-30D composite	-0.328	0.19	0.316	-0.432	87.3
Cu-10D coated NiCrB	-0.257	0.041	0.076	-0.577	18.8
Cu-30D coated NiCrB	-0.264	0.05	0.215	-0.337	22.9

3.4. EIS measurements

The EIS results (figures. 5-7 and Tables 5-7) indicate that one capacitive loop is clearly observed in the high-frequency region and a straight line (Warburg) in the low-frequency region is observed in the Nyquist plots of massive Cu, Cu-diamond uncoated composite, and Cu- diamond coated NiCrB composite electrodes as shown in figures 5-7(a-c). The capacitive loop is attributed to the polarization resistance (R_p), where the Warburg impedance is attributed to the diffusion of the anodic and cathodic reaction products from the solution to the electrode surface. The equivalent circuit that fits the Nyquist plots is shown in figure 8. R_s is the solution resistance between the reference and working electrodes, R_p is corresponding to the corrosion reaction at the metal substrate/solution interface, C_p is the capacitive loop and W is the Warburg impedance attributed to the mass transport during the corrosion reactions. It is found that the R_p values increased in Cu-diamond coated NiCrB composite electrodes compared to that of massive Cu and Cu-diamond uncoated composite electrodes, whereas the C_p values were found to be decreased (Tables 5-7). The decrease of capacity values for the Cu- diamond coated NiCrB composite electrodes was attributed to the good wetability of coated diamond with the Cu matrix acting as a barrier to the diffusion process. The obtaining result values obtained from EIS are in consistence with that obtained from Tafel lines.

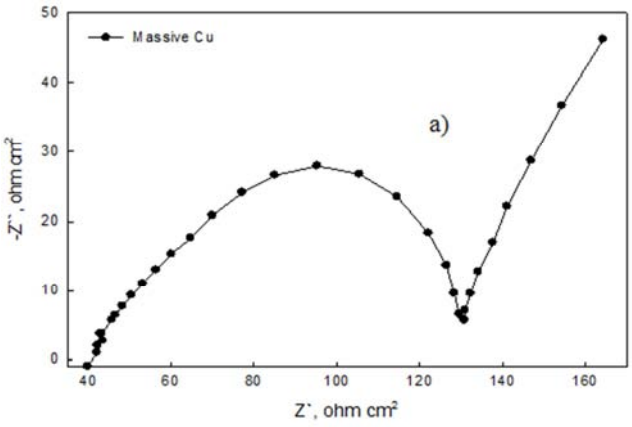

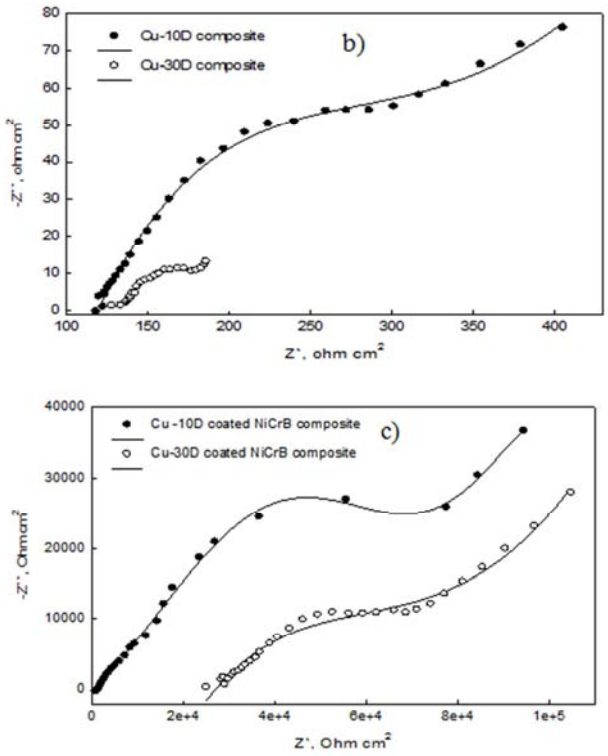

Figure 5. *Nyquist impedance patterns of a) massive Cu, b) Cu- diamond uncoated composite electrode, and c) Cu- diamond coated NiCrB composite electrode in 0.1 M HCl solution at 25°C at open circuit potential.*

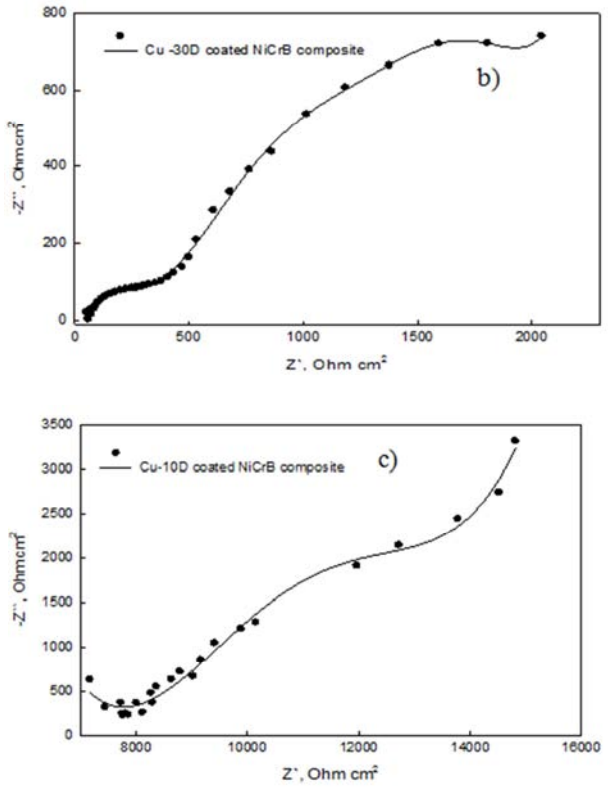

Figure 6. *Nyquist impedance patterns of a) massive Cu, b) Cu- diamond uncoated composite electrode, and c) Cu- diamond coated NiCrB composite electrode in 0.5 M NaOH solution at 25°C at open circuit potential.*

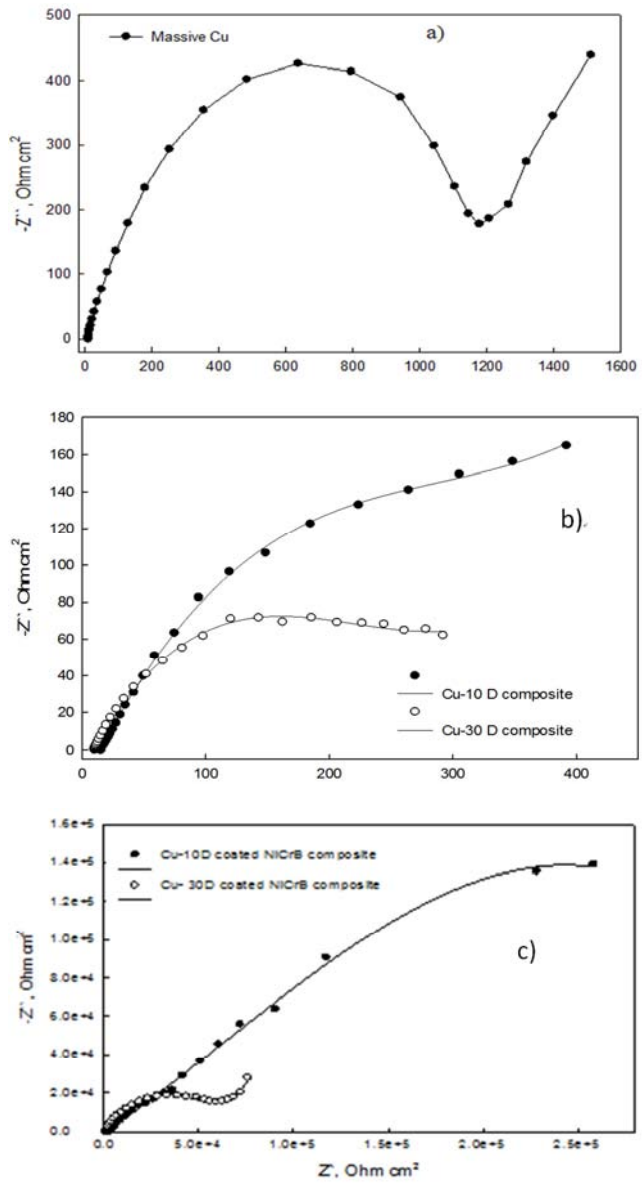

Figure 7. *Nyquist impedance patterns of a) massive Cu, b) Cu- diamond uncoated composite electrode, and c) Cu- diamond coated NiCrB composite electrode in 0.6 M NaCl solution at 25°C at open circuit potential.*

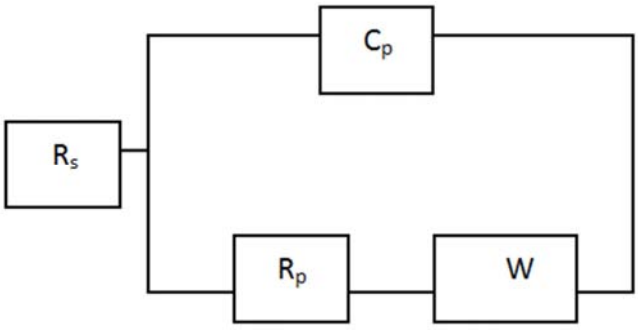

Figure 8. *The equivalent circuit R ([RW])C of Cu and Cu-composite samples.*

Table 5. *Electrochemical impedance spectroscopic data (EIS) for different Cu samples in 0.1 M HCl at open circuit potential at 25°C.*

Sample	**R_s, (Ω cm^2)**	**R_p, (Ω cm^2)**	**C_p F cm^{-2}**	**W (Ω cm^2)**	**N**
Massive Cu	48.8	71.9	$8.5x10^{-5}$	6.1	0.975
Cu-10D composite	128	134.4	$1.1x10^{-5}$	6.66	0.968
Cu-30D composite	125	61.2	$3.0x10^{-4}$	4.85	0.966
Cu-10D coated NiCrB	7616	47964	$9.69x10^{-7}$	$1.0x10^{5}$	0.887
Cu-30D coated NiCrB	7200	25800	$7.6x10^{-7}$	7.77×10^{4}	0.962

Table 6. *Electrochemical impedance spectroscopic data (EIS) for different Cu samples in 0.5 M NaOH at open circuit potential at 25°C.*

Sample	R_s, (Ω cm^2)	R_p, (Ω cm^2)	C_p F cm^{-2}	W (Ω cm^2)	N
Massive Cu	21.8	73.6	$8.9x10^{-4}$	5.03	0.975
Cu-10D composite	9.5	30.4	$1.7x10^{-2}$	17.8	0.999
Cu-30D composite	11.2	23.6	$1.2x10^{-4}$	5.58	0.979
Cu-10D coated NiCrB	7597.8	4630.5	$8.8x10^{-5}$	1783	0.963
Cu-30D coated NiCrB	460.2	1420.5	$3.6x10^{-5}$	925.7	0.973

Table 7. *Electrochemical impedance spectroscopic data (EIS) for different Cu samples in 0.6 M NaCl at open circuit potential at 25°C.*

Sample	**R_s, (Ω cm^2)**	**R_p, (Ω cm^2)**	**C_p F cm^{-2}**	**W (Ω cm^2)**	**N**
Massive Cu	41.3	988.8	$7.2x10^{-5}$	93.8	0.976
Cu-10D composite	23.5	193.4	$2.8x10^{-3}$	57.1	0.968
Cu-30D composite	19.5	169.8	$1.04x10^{-3}$	30.7	0.974
Cu-10D coated NiCrB	15680.8	198696	$7.66x10^{-6}$	$1.18x10^{4}$	0.977
Cu-30D coated NiCrB	4400.2	51900.5	$7.0x10^{-5}$	$0.94x10^{4}$	0.970

4. Conclusion

The corrosion behaviors of Cu/diamond composites (Cu-10 V_f % D, Cu-30 V_f % D, Cu-10 V_f % D coated NiCrB and Cu-30 V_f% D coated NiCrB) have been investigated through potentiodynamic polarization Tafel lines and EIS measurements in 0.6 M NaCl, 0.1 M HCl and 0.5 M NaOH solutions. The results of this investigation suggest some points, which can be summarized as follows:

- The corrosion behavior of Cu- diamond composites was related to the diamond content and the coating treatment.
- Analysis of potentiodynamic polarization and EIS results showed that a lower corrosion current density was recorded for massive Cu compared with that of Cu-diamond uncoated composite.
- The Cu-10 V_f% D coated NiCrB composite has a lower corrosion rate than the other investigated samples owing to the good wetability of the coated diamond with Cu matrix.
- Owing to its lower CTE and relatively lower corrosion rate, Cu-10 V_f% V_f % V_f % D coated NiCrB composite could be used as good heat dissipating materials in many industrial sectors.

References

[1] Xinjiang Z.; Pengyu D.; Benguo Z.; Shengyang T.; Zirun Y.; Yong C.; J. Alloys and Compounds, 2016, 671, 465.

[2] Issac D.; Ramasamy S.; Nadarajan M.; J. Materials Research and Technology; 2016, 54, 302.

[3] Sergey V; Kidalov and Fedor M. Shakhov; Materials; 2009, 2, 2467.

[4] Moustafa S. F; Zeitschrift Fuer Metallkunde; 1997, 88, 209.

[5] Moustafa S. F; Moustafa M. A.; El-Sahat O. A.; Mater. Lett.; 1996, 29, 37.

[6] Tavman I. H.; Powder Technol.; 1997, 91 (1), 63–67.

[7] Ruch P. W.; Beffort O.; Kleiner S.; Weber L.; Uggowitzer P. J; Compos. Sci. Technol., 2006, 66, 2677.

[8] Himbeault D. D.; Varin R. A.; Piekarski K.; Metall. Trans. A; 1988, 19A, 2109.

[9] Choo Seong-Hun; Lee Sunghak; and Kwon Soon-Ju; Metall. Trans. A; 1991, 30, 3131.

[10] Omayma A. G.; Abou Tabl M. H.; Abdel Hamid Z.; Mostafa S. F.; J. surf. and coat. Technol., 2006, 201, 1357.

[11] Moustafa S. F.; Abdel Hamid Z.; Fatma A. Morsy; Khalifa N. A.; Abdel Mouez F.; Natural Science, 2011, 3 (11), 936.

[12] Abdel Gawad O.; Chemistry Department, Faculty of Science, Cairo University, Ph. D thesis (2005).

[13] Shifler D. A.; Corros. Sci., 2005, 47, 2335.

[14] Metikos-Hukovic M; Babic R;, Corros. Sci., 2008, 51, 70.

[15] Khaled K. F.; Mater Chem. Phys., 2008, 112, 104.

[16] Zhang D. Q.; Cai Q. R.; He X. M.; Gao L. X.; Zhou G. D.; Mater. Chem. Phys., 2008, 112, 353.

[17] Abhijeet B.; Balasubramaniam R; Gupta M.; Corros. Sci., 2008, 50, 2423.

[18] Schultze J. W.; Lohrengel M. M.; Electrochim. Acta.; 2000, 45, 2499.

[19] Marcus P.; Electrochim. Acta., (1998, 43, 109.

[20] Qian S.; Newman R. C.; Cottis R. A.; Sieradzki K.; J Electrochem. Soc., 1990,137, 435.

[21] Milić S. M.; Antonijević M. M.; Šerbula S. M.; Bogdanović G. D; Corros. Eng. Sci. Technol., 2008, 43, 30.

[22] Kenneth K. A; Benjamin U. O.; Eng. Sci. and Technol., 2016, 19, 3, 1593.

[23] Kear G.; Barker B. D; Walsh F. F.; Corros. Sci.; 2004, 46, 109.

[24] Otmacic H.; Telegdi J.; Papp K.; Stupnisek Usac E.; Journal of Appl. Electrochem.; 2004, 34,5, 545.

[25] Deslouis C.; Tribollet B.; Mengoli G.; Musiani M. M.; Journal of Appl. Electrochem., 1988,18, 3, 374.

[26] Otmačić H.; Stupnišek-Lisac E.; Electrochim. Acta; 2003, 48, 985.

[27] Lee H. P.; Nobe K.; J. Electrochem. Soc.; 1986, 133, 2035.

[28] Abdel Hamid Z.; Abdel Mouez F.; Morsy F. A.; khalifa N. A.; International Journal of Engineering Practical Research; 2013, 2, 3, 112.

[29] Milošev, T. Kosec Mikić; M. Gaberšček, Electrochim. Acta, 2006, 52, 415.

[30] Abd El Haleem S. M.; Abd El Aal E. E.; Corros., 2006, 62, 121.

[31] Ferreira. J. P.; Rodrigues J. A.; da Fonseca I. T. E.; J. Solid State Electrochem.; 2004, 8, 260.

[32] Ribotta S. B.; La Morgia L. F.; Gassa L. M.; Folquer M. E.; J. Electroanal. Chem., 2008, 624, 262.

[33] Zaafarany I.; Boller H.; Current World Environment; 2009, 4 (2), 277.

[34] Levy M.; Chang F.; Blacksburg, Va, USA, 1981, p 33.

[35] El-Warraky; El-Shayeb H. A.; Sherif E. M.; Anti-Corros. Method and Materials, 2004, 51 (1), 52.

[36] Finsgar M.; Milosev I; Corros. Sci., 2010, 52, 2737.

[37] Zhang D. Q.; Gao L. X.; Zhou G. D; Lee K. Y.; Journal of Appl. Electrochem., 2008, 38, 1, 71.

[38] Appa Rao B. V.; Yakub Iqbal M. d.; Sreedhar B.; Electrochim. Acta; 2010, 55, 620.